Manipulation of spin reorientation transition by Au capping in body-centered cubic Ni(001) film

2008 J. Phys.: Condens. Matter 20 485010

(http://iopscience.iop.org/0953-8984/20/48/485010)

J. Phys.: Condens. Matter **20** (2008) 485010 (6pp) doi:10.1088/0953-8984/20/48/485010

Manipulation of spin reorientation transition by Au capping in body-centered cubic Ni(001) film

Dongyoo Kim, Jeong-hwa Yang and Jisang Hong

Department of Physics, Pukyong National University, Busman 608-737, Korea

E-mail: hongj@pknu.ac.kr

Received 12 September 2008, in final form 19 October 2008
Published 6 November 2008
Online at stacks.iop.org/JPhysCM/20/485010

Abstract

The thickness dependent magnetic properties of artificially prepared ultrathin body-centered cubic Ni films have been explored using the all electron full potential linearized augmented plane wave (FLAPW) method. We have considered two types of BCC Ni(001) films: (i) pure BCC Ni(001) and (ii) Au capped BCC Ni(001) in the range from 1 monolayer (ML) to 4 ML of Au capping coverage. The average magnetic moment of pure BCC Ni(001) is about 0.63 μ_B and a typical surface enhancement is found with a magnetic moment of 0.78 μ_B. In the presence of an Au capping layer, the magnetic moment of interface Ni is strongly suppressed to approximately 0.5 μ_B and this causes a reduction of average magnetic moment. Nevertheless, the Au adlayer has no meaningful induced magnetic moment. The BCC pure Ni(001) films always have in-plane magnetization up to 11 ML, but very interestingly the Au/Ni(001) shows a thickness dependent spin reorientation transition (SRT) from in-plane to perpendicular to the film surface. However, the thickness dependent SRT shows very irregular behavior. In addition, the calculated x-ray absorption spectroscopy (XAS) and x-ray magnetic circular dichroism (XMCD) have been presented.

(Some figures in this article are in colour only in the electronic version)

1. Introduction

In thin film magnetism, the materials composed of typical 3d transition metal elements have been extensively explored. As is well known, Fe, Co, and Ni have body-centered-cubic (BCC), hexagonal-close-packed (HCP), and face-centered-cubic (FCC) crystal structures in bulk mode, respectively. To date, the fundamental magnetic properties of these materials in bulk state are well understood. On the other hand due to advanced atomic manipulation techniques, it is possible to create artificial nanostructures which do not exist in nature. For instance, Fe and Co can maintain the FCC phase under certain conditions although they have BCC and HCP crystal structures in bulk structure [1–3]. This means that the thermodynamically stable crystal structure can be tailored and it may bring new opportunities to utilize the noble magnetic properties for potential magnetic device applications. However, there was no report on BCC type Ni and it has long been remained an intriguing issue to grow BCC Ni until recently although the magnetic properties of BCC Ni have been studied using first principles method [4, 5]. One may see that many studies for the BCC Ni on Fe(001) have been presented [6–9], but in this case it is obvious that the magnetism of BCC Ni is affected by the hybridization with magnetic Fe surface.

In order to understand the intrinsic magnetism of BCC Ni, not affected by magnetic materials, one needs to grow BCC Ni on a non-magnetic surface. Interestingly, it has been demonstrated that the bulk like BCC Ni can be epitaxially grown on a GaAs(001) surface with a lattice constant of $a = 0.282$ nm [10, 11]. According to the report by Tian *et al* [10], the Ni/GaAs(001) manifests a magnetic moment about 0.53 μ_B and the bulk like BCC Ni has an in-plane cubic magnetocrystalline anisotropy energy of 4.7×10^5 ergs cm^{-3}. On the theoretical side, several first principles calculations have been performed to reveal the magnetic properties of BCC Ni [12–14]. These theoretical studies show that the lattice distortion of BCC Ni does not substantially influence the magnetic moment [12] and the calculated magnetic moment

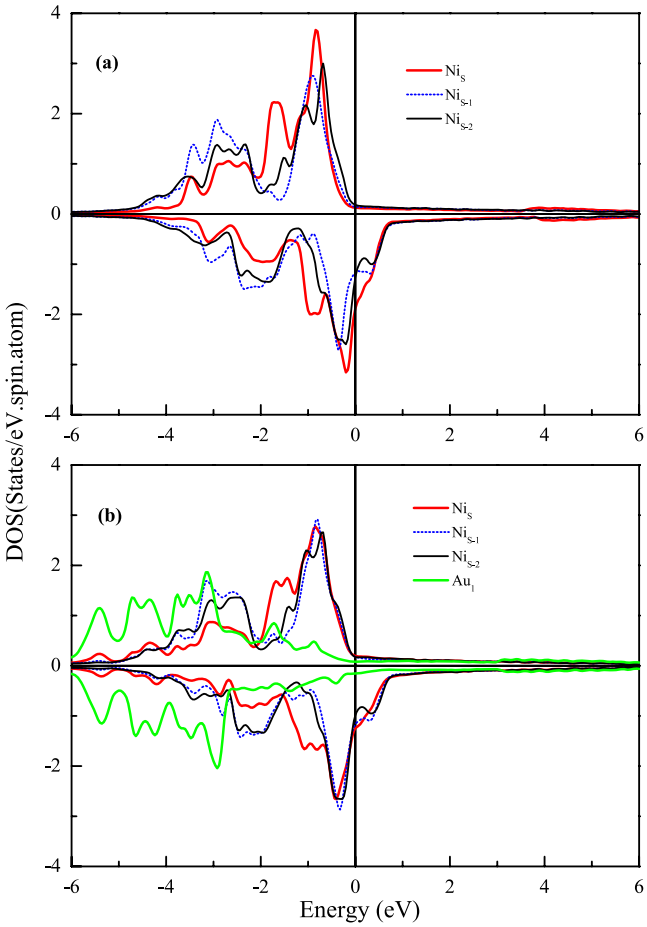

Figure 1. DOS of (a) pure BCC Ni and (b) Au(1 ML)/Ni (11 ML). Here, the thickness of Ni is 11 ML.

does not deviate significantly from the experimentally found value. In addition, a theoretical study for magnetic anisotropy of bulk like BCC Ni is presented [13].

Despite all these efforts, to the best of our knowledge so far, no one has ever studied the magnetic properties of ultrathin BCC Ni films. In this respect, we aim to investigate the thickness dependent magnetic anisotropy both of ultrathin pure BCC Ni and Au capped Ni films. In particular, it will be of interest to determine whether one can find a perpendicular magnetic anisotropy (PMA) or a thickness dependent spin reorientation transition (SRT) phenomenon. From the experimental point of view, x-ray magnetic circular dichroism (XMCD) is well known as a useful tool to extract element specific magnetic information. We will thus present theoretically calculated XAS and XMCD results as well.

2. Numerical method

The thin film version of full potential linearized augmented plane wave (FLAPW) method is employed in our calculations. Therefore, no shape approximation is assumed in the charge, potential, and wavefunction expansions [15–17]. We treat the core electrons fully relativistically, and the spin–orbit interactions among valence electrons are dealt with second variationally [18]. The generalized gradient approximation is used to describe the exchange correlation [19]. Spherical harmonics with $l_{\max} = 8$ are used to expand the charge, potential, and wavefunctions in the muffin tin region. Energy cut offs of 225 and 13.7 Ry are implemented for the plane wave star function and basis expansions in the interstitial region. We use 210 k-mesh points during the entire course of the calculations discussed in this report. Since it is found that BCC Ni grown on GaAs(001) has a lattice constant of 0.282 nm, we employ the same lattice parameters in the lateral direction. To investigate the effect of Au capping on the thickness dependent magnetic anisotropy of the Ni film, we assume that the Au adlayer can also be grown on BCC Ni pseudomorphically, while the vertical positions of all constituents are optimized via force and total energy minimization procedures. Here, we have considered the range from 5 to 11 ML Ni thickness and the Au capping layer is increased up to 4 ML coverage.

3. Results and discussions

We first show the optimized atomic structure and magnetic moments of pure BCC Ni and Au capped systems in table 1. The surface Ni layer is represented by Ni$_S$, and Ni$_{S-1}$ stands for the subsurface layer. Au$_i$ represents the position of the Au adlayer measured from Ni$_S$. Note that we have only displayed the optimized vertical distances of the Au/Ni(11 ML) system. In other Au/Ni films, there no physically meaningful change was found (not shown here). In pure Ni(001) films, one can see that the calculated vertical distances are close to the bulk value for the inner layers, but an inward relaxation is observed in the surface layer. In the Au/Ni(11 ML), the interlayer distances are suppressed by less than 0.1 Å near the interface region, whereas the distances of the inner layers are only slightly changed.

In tables 2 and 3, we present the calculated spin and orbital magnetic moments, respectively. The average spin magnetic moment of pure Ni is in the range from 0.63 to 0.66 μ_B and this is somewhat larger than that found in bulk like BCC Ni [10]. The increased average magnetic moment is obviously due to the well known surface enhancement as one can see from the table 2. In the presence of the Au capping layer, the average magnetic moment is suppressed to about 0.57–0.58 μ_B. The magnetic moment of Ni$_S$ is significantly affected by the Au adlayer and this contributes to the reduction of average magnetic moment. It is observed that the magnetic moment of Ni is almost unchanged after 2 ML Au capping. We have found the same trends in other systems although only the results of Au/Ni(11 ML) are shown in table 2. For the orbital magnetic moment a similar behavior is observed although it is one order of magnitude smaller than that for the spin moment.

We now discuss the density of states (DOS) of pure BCC Ni and Au/Ni films. In figures 1(a) and (b), the DOS of pure Ni(11 ML) and Au/Ni(11 ML) are presented, respectively (the first few layers are shown). One can see that the majority spin states are quite small at the Fermi level, while the minority states are sizable. All the Ni layers manifest similar behaviors in both majority and minority spin states at the Fermi level. From figure 1(a), it is found that the number of holes in the

Table 1. Optimized interlayer distances (in Å) of pure BCC and Au/Ni films.

	Ni				Au			
Thickness	5 ML	7 ML	9 ML	11 ML	1 ML	2 ML	3 ML	4 ML
$d(Ni_{S-5}–Ni_{S-4})$				1.40	1.39	1.39	1.38	1.38
$d(Ni_{S-4}–Ni_{S-3})$			1.37	1.38	1.39	1.37	1.38	1.36
$d(Ni_{S-3}–Ni_{S-2})$		1.40	1.37	1.41	1.40	1.37	1.36	1.37
$d(Ni_{S-2}–Ni_{S-1})$	1.43	1.40	1.40	1.44	1.37	1.35	1.35	1.35
$d(Ni_{S-1}–Ni_S)$	1.34	1.36	1.32	1.37	1.36	1.33	1.33	1.33
$d(Ni_S–Au_1)$					1.76	1.75	1.75	1.75
$d(Au_1–Au_2)$						2.21	2.23	2.23
$d(Au_2–Au_3)$							2.22	2.23
$d(Au_3–Au_4)$								2.21

Table 2. Calculated spin magnetic moments (in μ_B) of pure Ni film and Au capped Ni(11 ML) films.

	Ni				Au			
Thickness	5 ML	7 ML	9 ML	11 ML	1 ML	2 ML	3 ML	4 ML
Ni_{S-5}				0.57	0.60	0.58	0.57	0.57
Ni_{S-4}			0.61	0.60	0.58	0.59	0.60	0.59
Ni_{S-3}		0.53	0.56	0.56	0.60	0.59	0.58	0.59
Ni_{S-2}	0.53	0.58	0.57	0.58	0.55	0.55	0.56	0.55
Ni_{S-1}	0.64	0.65	0.66	0.67	0.64	0.59	0.58	0.59
Ni_S	0.78	0.78	0.78	0.79	0.55	0.50	0.49	0.49

Table 3. Calculated orbital magnetic moments (in μ_B) of pure Ni film and Au capped Ni(11 ML) films.

	Ni				Au			
Thickness	5 ML	7 ML	9 ML	11 ML	1 ML	2 ML	3 ML	4 ML
Ni_{S-5}				0.04	0.04	0.04	0.04	0.04
Ni_{S-4}			0.05	0.05	0.04	0.04	0.04	0.04
Ni_{S-3}		0.04	0.04	0.04	0.04	0.05	0.05	0.05
Ni_{S-2}	0.03	0.04	0.04	0.04	0.04	0.03	0.03	0.03
Ni_{S-1}	0.05	0.05	0.05	0.05	0.05	0.05	0.05	0.05
Ni_S	0.08	0.09	0.08	0.08	0.04	0.03	0.04	0.03

Table 4. Calculated magnetic anisotropy energies per Ni atom (in μeV).

Au coverage	0	1 ML	2 ML	3 ML	4 ML
K_1					
Ni(5 ML)	0.52	0.04			
Ni(7 ML)	−0.11	4.8			0.8
Ni(9 ML)	−0.18				
Ni(11 ML)	−0.16		−2.73	3.82	2.06
K_U					
Ni(5 ML)			151	150	89
Ni(7 MN)			68	35	
Ni(9 ML)		75	70	46	44
Ni(11 ML)		19.7			

majority spin bands are almost the same, whereas the Ni_S has more holes in the minority spin bands compared with those in other atoms. Thus, one can see well known surface enhancement in Ni_S. In figure 1(b), we display the DOS of the Au(1 ML)/Ni(11 ML) film. As shown, the main features of the DOS of the Ni layers are unchanged even in the presence of Au capping layers except for the DOS of Ni_S and this can nicely account for the trends in table 2. In the DOS of Ni_S, it is seen that the minority spin state is shifted to the left compared with that in the pure case and this causes reduction of empty holes, while the majority spin holes are unchanged. Consequently, we can see a suppressed surface magnetic moment in Ni_S. It is clear that this change is due to the hybridization with the Au atom as one can see from the DOS of the Au adlayer in figure 1(b) (green line). We have also explored the DOS features for other systems and have obtained very similar trends although they are not presented here.

The main issue of this report is to explore the thickness dependent magnetic anisotropy of ultrathin BCC Ni and Au/Ni films. The magnetic moment is simply a difference in the number of majority and minority spin electrons below the Fermi level and it has nothing to do with the wavefunction character of the occupied states. However the magnetic anisotropy arising from spin–orbit coupling depends on the wavefunction feature and this may indicate that the direction of magnetization is strongly affected by subtle changes in the underlying electronic structure. Since the magnitude of the spin–orbit interaction is usually small, it is necessary to employ very accurate numerical methods to deal with the spin–orbit interaction resulting from the relativistic effect. To this aim, we use the torque method [20]. It is known that the torque method provides very stable results even with fewer k-points as compared to methods that employ different

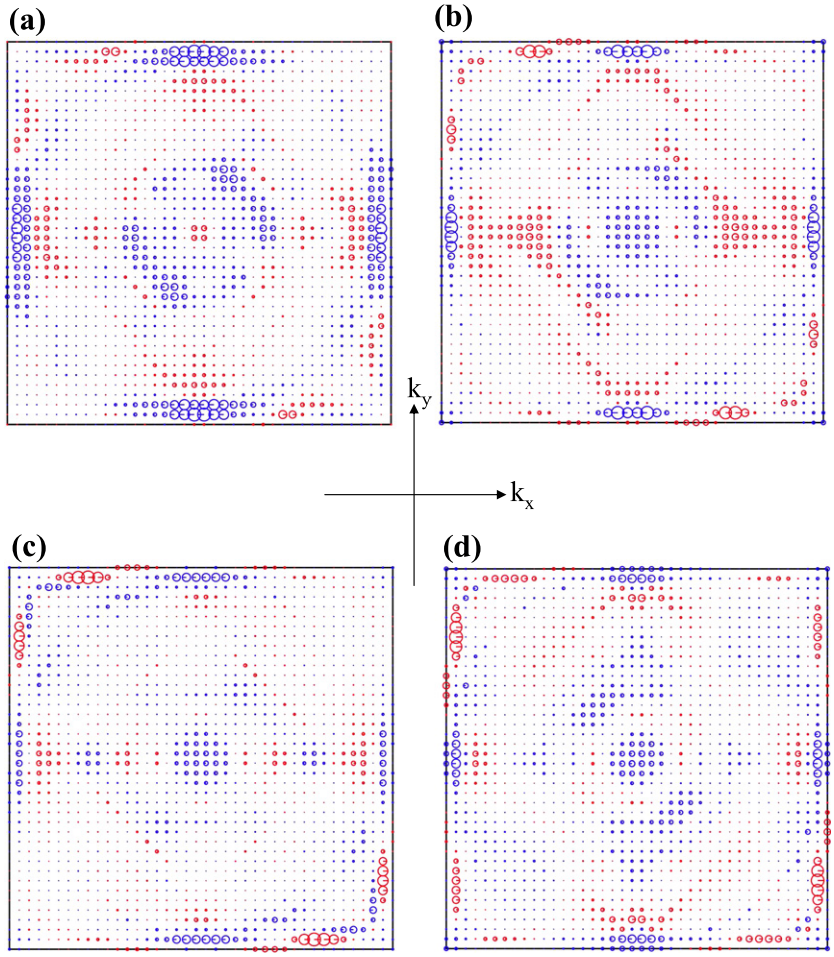

Figure 2. Distribution of magnetic anisotropy over two-dimensional BZ; (a) pure BCC Ni(11 ML), (b) Au(1 ML)/Ni(11 ML), (c) Au(2 ML)/Ni(11 ML) and (d) Au(3 ML)/Ni(11 ML).

schemes since the torque method calculates the magnetic anisotropy energy (MAE) via expectation values of the angular derivative of the spin–orbit Hamiltonian. We will calculate both $E_1 = E_{100} - E_\perp$ and $E_2 = E_{110} - E_\perp$ where E_{100} and E_{110} stand for the total energy when the direction of magnetization points to the (100) and (110) direction with in-plane magnetization, respectively, while $E_\perp$ means the total energy for the perpendicular magnetization. Using this, we can find a cubic MAE $K_1 = E_1 - E_2 = E_{100} - E_{110}$ for in-plane magnetization systems and an uniaxial perpendicular MAE $K_U = E_{100(110)} - E_\perp$. A negative K_1 stands for in-plane magnetization in the (100) direction, while a positive K_1 means in-plane magnetization along the (110) direction. The calculated results are shown in table 4. Here, it should be remarked that we have the same MAE for both 300 k-points and 210 k-points. Thus, the numerical convergence issue is satisfied. It is well known that the FCC Ni/Cu(001) film manifests an SRT from in-plane to perpendicular to the film surface at a thickness of 7–10 ML and the magnetic anisotropy can also be tuned due to the oxygen effect [21]. Here, as shown above, there is no such thickness dependent SRT from the in-plane to perpendicular direction in ultrathin BCC Ni films at least up to 11 ML thickness. One can see that the 5 ML Ni film has a magnetization along the (110) direction and all other BCC Ni films have an easy axis along the (100) direction. Very interestingly, the Au capped ultrathin BCC Ni films display quite different magnetic anisotropy from that of pure Ni films. For instance, the Au(1 ML)/Ni(5 ML) still shows in-plane magnetization, but the magnitude of cubic anisotropy is greatly changed. In Au(2 ML)/Ni(5 ML), a large perpendicular magnetic anisotropy of $K_U = 151$ μeV per Ni atom is realized. In Au/Ni(11 ML), we also see SRT from the in-plane, i.e. (100) direction, magnetization to the perpendicular direction at 1 ML Au coverage and then the direction of magnetization changes from perpendicular to the film surface to the (110) direction (in-plane magnetization) upon adding more Au layers. The calculated results definitely show that the influence of interface contribution plays an essential role in determining the direction of magnetization, but the overall behaviors are not consistent with increasing Au capping. Therefore, the conventional interpretation in terms of competition among surface, interface, and volume parts may not be applicable to this ultrathin film structure because it is not possible to clearly separate each contribution in a few monolayer thickness.

On the theoretical side, the generalized relation between magnetic anisotropy and orbital anisotropy has been proposed by Van der Laan [22], but this correlation is not yet clear [23]. We therefore present the overall distribution of magnetic

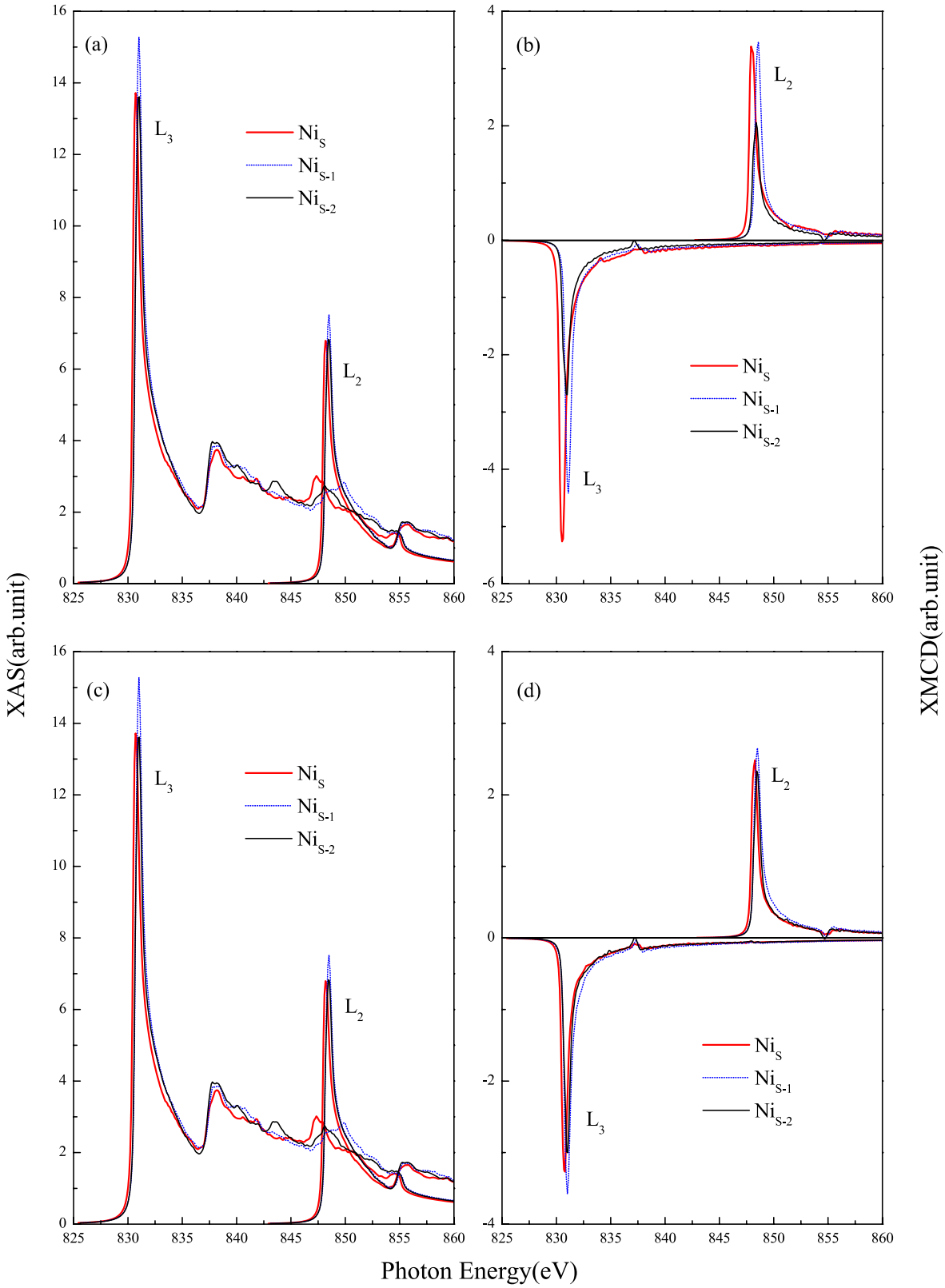

Figure 3. Calculated XAS and XMCD; (a) XAS of pure Ni(11 ML), (b) XMCD of pure Ni(11 ML), (c) XAS of Au(1 ML)/Ni(11 ML) and (d) XMCD of Au(1 ML)/Ni(11 ML).

anisotropy over two-dimensional Brillouin zone (BZ). If the spin–orbit interaction between the occupied and unoccupied state at a give k-point has a contribution to perpendicular magnetization, it is represented by a red circle (light gray), while the blue circle (dark gray) is for the contribution to in-plane magnetization. The magnitude of magnetic anisotropy is proportional to the size of circle. Of course, the net magnetic anisotropy energy results from the summation of each k-point

contribution. As a representative illustration for the MAE distribution, the distributions of 11 ML pure Ni, Au(1 ML)/Ni, Au(2 MN)/Ni, and Au(3 ML)/Ni are shown in figure 2. As shown in figure 2(a) for 11 ML of pure Ni film, the strong in-plane contributions to the magnetic anisotropy mainly arise from the 2D BZ boundary and around the circumference radius of $\pi/2a$. In the presence of 1 ML of Au capping as in figure 2(b), the in-plane contributions from the ZB boundary are significantly suppressed. On the other hand, one can see a greater contribution to the perpendicular magnetization approximately in the line of the k_x direction. As a result, a perpendicular magnetization to the film surface is achieved. Adding more Au layers, one can see different behavior and this implies that the character of the wavefunction is greatly modified. One may attempt to analyze the thickness dependent MAE via a wavefunction character study; for instance a simple interpretation such as Γ point analysis in the bulk FeCo alloy [24]. In the present case, one can see that many k-points have a similar magnitude of magnetic anisotropy energy contributing to the perpendicular direction or in-plane magnetization. Since there is no single dominant k-point contributing to the magnetic anisotropy, it is not possible to do such a single k-point wavefunction analysis. Instead, it has been found that the overall effect results from the competition among many counteracting contributions.

In figure 3, the calculated x-ray absorption spectrum (XAS) and x-ray magnetic circular dichroism (XMCD) are presented. Here, we only consider dipole transition assuming rigid core–hole relaxation. Thus, the exact peak position should be shifted if one compares the calculated results with experimental data. The Doniach–Sunjic shape [25] with 0.12 eV for life time broadening. We show the results of pure Ni and Au/Ni with 11 ML film thickness. The XAS and XMCD of pure Ni and Au capped systems are almost identical although the intensity of XMCD in Au/Ni is slightly suppressed. Due to the rather simple unoccupied DOS above the Fermi level in figure 1, we have a well separated single peak L edge XMCD. The peak position of the Ni_S L edge is shifted to the left and this can be understood from the calculated DOS in figure 1 since the minority spin DOS of N_S is shifted to the left. The calculated orbital magnetic moment of Ni_S is 0.09 μ_B for pure Ni and it is reduced to 0.04 μ_B due to Au(1 ML) capping. We have found about 0.04 μ_B for the inner layers. Please note that the spectral shapes of the XAS and XMCD for other systems are not presented here, but we have found that there are no physically meaningful changes.

4. Summary

In conclusion, we have investigated the thickness dependent magnetic anisotropy of ultrathin pure BCC Ni and Au/Ni systems. The magnetic moment of the interface Ni is significantly suppressed in the presence of an Au adlayer, whereas the magnetic states of the inner layers are not changed. It has been observed that the BCC Ni always has in-plane magnetization up to 11 ML thickness. Very interestingly the Au/Ni manifests a thickness dependent SRT according to the Au coverage, but there is no consistent trend. The calculated XAS and XMCD have a well separated single peak L edge and this can be easily understood from the simple unoccupied DOS as shown. Since this is the first theoretical report on the thickness dependent SRT in an ultrathin BCC Ni film, we hope that the results will stimulate further experimental verification.

Acknowledgments

This work was supported by the Korea Research Foundation Grant funded by the Korean Government (MOEHRD, Basic Research Promotion Fund) (KRF-2007-331-C00102).

References

[1] Prinz G A 1985 *Phys. Rev. Lett.* **54** 1051
[2] Qian D, Jin X F, Barthel J, Klaua M and Kirschner J 2001 *Phys. Rev. Lett.* **87** 227204
[3] Tsunoda Y 1989 *J. Phys.: Condens. Matter* **1** 10427
[4] Moruzzi V L 1986 *Phys. Rev. Lett.* **57** 2211
[5] Moruzzi V L, Marcus P M, Schwarz K and Mohn P 1986 *Phys. Rev.* B **34** 1784
[6] Heinrich B, Purcell S T, Dutcher J R, Urquhart K B, Cochran J F and Arrott A S 1988 *Phys. Rev.* B **38** 12879
[7] Wang Z Q, Li Y S, jona F and Marcus P M 1987 *Solid State Commun.* **61** 623
[8] Bland J A C, Bateson R D, Johnson A D, Heinrich B, Celinski Z and Lauter H J 1991 *J. Magn. Magn. Mater.* **93** 331
[9] Lin T, Schwickert M M, Tomaz M A, Chen H and Harp G R 1999 *Phys. Rev.* B **59** 13911
[10] Tian C S, Qian D, Wu D, He R H, Wu Y Z, Tang W X, Yin L F, Shi Y S, Dong G S, Jin X F, Jin X,M, Liu F Q, Qian H J, Sun K, Wang L M, Rossi G, Qiu Z Q and Shi J 2005 *Phys. Rev. Lett.* **94** 137210
[11] Tang W X, Qian D, Wu D, Wu Y Z, Dong G S, Jin X F, Chen S M, Jiang X M, Zhang X X and Zhang Z 2002 *J. Magn. Magn. Mater.* **240** 404
[12] Khmelevskyi S and Mohn P 2007 *Phys. Rev.* B **75** 012411
[13] Etz C, Vernes A, Szunyogh L and Weinberger P 2008 *Phys. Rev.* B **77** 064420
[14] Guo G Y and Wang H H 2000 *Chin. J. Phys.* **38** 949
[15] Wimmer E, Krakauer H, Weinert M and Freeman A J 1981 *Phys. Rev.* B **24** 864
[16] Weinert M, Wimmer E and Freeman A J 1982 *Phys. Rev.* B **26** 4571
[17] Weinert M 1981 *J. Math. Phys.* **22** 2433
[18] Koelling D D and Hamon B N 1977 *J. Phys. C: Solid State Phys.* **10** 3107
[19] Perdew J P, Burke K and Ernzerhof M 1996 *Phys. Rev. Lett.* **77** 3865
[20] Wang X D, Wu R Q, Wang D S and Freeman A J 1996 *Phys. Rev.* B **54** 61
[21] Hong Jisang, Wu R Q, Lindner J, Kosubek E and Baberschke K 2004 *Phys. Rev. Lett.* **92** 147202
[22] Van der Laan G 1998 *J. Phys.: Condens. Matter* **10** 3239
[23] Galanakis I, Alouani M and Dreyssé H 2000 *Phys. Rev.* B **62** 6475
[24] Burkert T, Nordström L, Eriksson O and Heinonen O 2004 *Phys. Rev. Lett.* **93** 027203
[25] Doniach S and Sunjic M 1970 *J. Phys. C: Solid State Phys.* **3** 285